Near-Perfect-Reconstruction Pseudo-QMF Banks

Truong Q. Nguyen, *Member, IEEE*

***Abstract*— A novel approach to the design of M-channel pseudo-quadrature mirror filter (QMF) banks is presented. In this approach, the prototype filter is constrained to be a linear-phase spectral-factor of a $2M$th band filter. As a result, the overall transfer function of the analysis/synthesis system is a delay. Moreover, the aliasing cancellation (AC) constraint is derived such that all the significant aliasing terms are canceled. Consequently, the aliasing level at the output is comparable to the stopband attenuation of the prototype filter. In other words, the only error at the output of the analysis/synthesis system is the aliasing error which is at the level of stopband attenuation. Using this approach, it is possible to design a pseudo-QMF bank where the stopband attenuation of the analysis (and thus synthesis) filters is on the order of -100 dB. Moreover, the resulting reconstruction error is also on the order of -100 dB. Several examples are included.**

I. Introduction

DIGITAL filter banks are used in a number of communication applications such as subband coders for speech signals [1]–[3], frequency domain speech scramblers [4], and image coding [5]–[7]. Fig. 1(a) illustrates a typical M-channel maximally decimated parallel filter bank where $H_k(z)$ and $F_k(z), 0 \leq k \leq M-1$ are analysis and synthesis filters, respectively (only finite impulse response (FIR) filters are considered in this paper). The analysis filters $H_k(z)$ channelize the input signal $x(n)$ into M subband signals, which are in turn decimated by M. In speech comparison and transmission applications [1]–[4], these M subband signals are encoded and transmitted. At the receiving end, the M subband signals are decoded, interpolated, and recombined using a set of synthesis filters $F_k(z)$. The decimator, which decreases the sampling rate of the signal, and the interpolator, which increases the sampling rate of the signals, are denoted by the down-arrowed boxed in the figure [2], respectively. The theory for perfect reconstruction has recently been established [8]–[12].

Recently, the perfect-reconstruction (PR) cosine-modulated filter bank has emerged as an optimum filter bank with respect to implementation cost and design ease [13]–[16], [33]–[35]. The impulse responses of the analysis and synthesis filters $h_k(n)$ and $f_k(n)$ are cosine-modulated versions of the

Manuscript received April 17, 1992; revised February 8, 1993. This work was supported by the Department of Defense and the Department of the Air Force under Contract F19628-90-C-0002. The associate editor coordinating the review of this paper and approving it for publication was Prof. Sergio D. Cabrera.

The author is with the Lincoln Laboratory, Massachusetts Institute of Technology, Lexington, MA 02173.

IEEE Log Number 9213291.

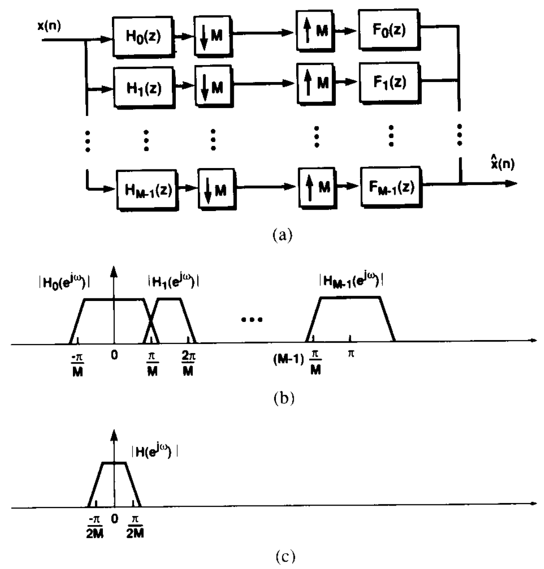

Fig. 1. (a) M-channel maximally decimated filter bank; (b) typical ideal responses of the analysis filters $H_k(z)$; (c) typical ideal response of the prototype filter $H(z)$.

prototype filter $h(n)$ [14]. In other words,

$$\begin{cases} h_k(n) = 2h(n)\cos\left((2k+1)\dfrac{\pi}{2M}\left(n-\dfrac{N-1}{2}\right)+(-1)^k\dfrac{\pi}{4}\right), \\ f_k(n) = 2h(n)\cos\left((2k+1)\dfrac{\pi}{2M}\left(n-\dfrac{N-1}{2}\right)-(-1)^k\dfrac{\pi}{4}\right), \end{cases}$$
$$\begin{cases} 0 \leq n \leq N-1 \\ 0 \leq k \leq M-1 \end{cases} \tag{1}$$

where N is the length of $h(n)$. It is shown in [14] that the $2M$ polyphase components of the prototype filter $H(z)$ can be grouped into M power-complementary pairs where each pair is implemented to minimize the stopband attenuation of the prototype filter. As demonstrated in [14], it is possible to design a 17-channel PR cosine-modulated filter bank with -40 dB stopband attenuation. This optimization procedure, however, is very sensitive to changes in the lattice coefficients because of the highly nonlinear relation between the prototype filter $h(n)$ and the lattice coefficients. As a result, a PR cosine-modulated filter bank with high stopband attenuation (on the order of -100 dB) is very difficult to design. For more than two channels, no example of a PR cosine-modulated filter bank, where its prototype filter has -100 dB attenuation, has yet been found. Consequently, in order to design a filter bank with high attenuation, it is judicious to relax the PR condition. In other words, it is sufficient (in the practical sense) to design a filter bank where the reconstruction error is small (on the order of -100 dB).

The pseudo-QMF banks belong to the family of modulated filter banks. Pseudo-QMF theory is well known [20]–[23] and is widely used. As with the PR cosine-modulated filter bank (1), the analysis and synthesis filters are cosine-modulated versions of a prototype filter. Since the desired analysis and synthesis filters have narrow transition bands and high stopband attenuation, the overlap between nonadjacent filters is negligible. Moreover, it is shown in [20] that the significant aliasing terms from the overlap of the adjacent filters are cancelled by the filter designs. The prototype filter $H(z)$ is found by minimizing an objective function consisting of the stopband attenuation and the overall distortion. As shown in [20]–[23], although it is possible to obtain a pseudo-QMF bank with high attenuation, the overall distortion level might be high (on the order of -40 dB). In summary, the overall distortion of the pseudo-QMF bank is not sufficiently small enough for application where a -100 dB error level is required.

The modulation schemes in the cosine-modulated filter banks [14], the modulated lapped transform [34], the Princen/Bradley filter bank [35], the pseudo-QMF bank [20]–[23], and the proposed NPR Pseudo-QMF bank use consine modulation with different phase factors. The first three filter banks are PR filter banks, whereas the last two are NPR filter banks. The NPR filter bank proposed here has no restriction on the filter's length, and it sacrifices some aliasing at the output for better stopband attenuation.

Reference [15] presents an approach to pseudo-QMF design which does not involve any optimization. The prototype filter of an M-channel filter bank is obtained as a spectral factor of a $2M$th band filter [24], [25]. Since the procedure does not guarantee that $H(z)$ is a linear-phase filter, the overall transfer function $T_0(z)$ of the analysis/synthesis system is an approximately flat magnitude response in the frequency region $\epsilon \leq \omega \leq (\pi - \epsilon)$. Here, ϵ depends on the transition bandwidth of the prototype filter and $0 \leq \epsilon \leq \pi/(2M)$. Furthermore, since the prototype filter is a spectral factor of a $2M$th band filter, designing a filter bank with high attenuation is difficult because of the sensitivity in the spectral factor algorithm. Moreover, the overall distortion can be large near $\omega = 0$ and $\omega = \pi$.

In summary, designing a filter bank with high stopband attenuation ($\simeq -100$ dB), small overall distortion ($\simeq -100$ dB), and small aliasing ($\simeq -100$ dB) is a formidable task. As discussed above, the PR cosine-modulated filter bank is too restrictive and the pseudo-QMF bank is too loose in its constraints. Consequently, the above filter banks, i.e., the PR cosine-modulated filter bank [14], [16] and the spectral-factorized pseudo-QMF filter bank [20], [15], do not yield satisfactory results. In this paper, an algorithm is described to obtain the pseudo-QMF bank with the following properties:

1) The analysis and synthesis filters have high stopband attenuation ($\simeq -100$ dB).
2) Overall distortion and alias level are small ($\simeq -100$ dB).

In Section II, a brief summary of the pseudo-QMF bank and the spectral factorization approach to the pseudo-QMF bank is presented. The new approach is derived fully in Section III. Moreover, it is shown that the overall distortion of the new pseudo-QMF bank is a delay, i.e., there is no magnitude or phase distortion. Furthermore, the aliasing level is comparable to the stopband attenuation. (Here, the aliasing level and the stopband attenuation are defined to be the peak aliasing error at the output and the peak stopband attenuation of the prototype filter, respectively.) In other words, the only error at the output is the aliasing error, which is very small. Several examples are given and their frequency responses plotted in Section IV.

Notation Used in the Paper: The variable ω is used as the frequency variable, whereas the term "normalized frequency" is used to denote $f = \omega/(2\pi)$. Boldfaced quantities denote matrices and column vectors, with upper case used for the former and lower case for the latter, as in $\boldsymbol{A}, \boldsymbol{h}(z)$, etc. The superscript t stands for matrix transposition. $\tilde{H}(z) \triangleq H(z^{-1})$. Moreover, $[\boldsymbol{A}]_{k,l}$ and $[\boldsymbol{h}]_k$ represent the (k,l)th and kth element of the matrix $\boldsymbol{A}$ and vector $\boldsymbol{h}$, respectively. The $k \times k$ identity matrix is denoted as $\boldsymbol{I}_k$; the $k \times k$ "reverse operator" matrix J_k is defined to be

$$J_k = \begin{pmatrix} 0 & \cdots & 0 & 1 \\ 0 & \cdots & 1 & 0 \\ \vdots & \ddots & \vdots & \vdots \\ 1 & \cdots & 0 & 0 \end{pmatrix}_k$$

and $\boldsymbol{V}$ is $\boldsymbol{V} = \begin{pmatrix} \boldsymbol{I}_{mM+m_1} & \boldsymbol{0} \\ \boldsymbol{0} & \frac{1}{2} \end{pmatrix}$. The subscripts of I_k and J_k are often omitted if they are clear from the context. W_M is defined as $e^{-j2\pi/M}$. Unless mentioned otherwise, W is the same as W_{2M}.

II. Review of Pseudo-QMF Banks

Consider the filter bank in Fig. 1(a) where the ideal frequency responses of the filters $H_k(z)$ are shown in Fig. 1(b). It can be verified that the reconstructed signal $\hat{X}(z)$ is [10]

$$M\hat{X}(z) = X(z)T_0(z) + \sum_{l=1}^{M-1} X(zW_M^l)T_l(z) \qquad (2)$$

where

$$T_l(z) = \sum_{k=0}^{M-1} F_k(z)H_k(zW_M^l). \qquad (3)$$

From (2), it is clear that $T_0(z)$ is the overall distortion transfer function and $T_l(z), l \neq 0$ is the $(M-1)$ aliasing transfer function corresponding to $X(zW_M^l)$. Thus, for a PR system,

$$\begin{cases} T_0(z) = z^{-n_0} \\ T_l(z) = 0. \qquad 1 \leq l \leq M-1 \end{cases} \qquad (4)$$

where n_0 is a positive integer. From a practical perspective, the above conditions in (4) are too restrictive; it is sufficient to design the filter bank such that $T_0(z)$ is linear phase and

$$\begin{cases} |T_0(e^{j\omega})| = 1 + \delta_1, \\ |T_l(e^{j\omega})| = \delta_2, \qquad 1 \leq l \leq M-1 \end{cases} \qquad (5)$$

where δ_1 and δ_2 are small numbers ($\simeq -100$ dB). In the examples presented later, $\delta_1 \leq 1 \times 10^{-12}$ and δ_2 is comparable to the stopband attenuation.

A. Pseudo-QMF Banks [20]

Most of the material in this section can also be found in [20], [14], [16]. The main properties are summarized in the following:

1) The linear-phase prototype filter is designed to approximate the frequency response in Fig. 1(c). A weighted objective function consisting of the stopband attenuation and the overall magnitude distortion is minimized.

2) The analysis and synthesis filters $H_k(z)$ and $F_k(z)$ are obtained by the modulation of $H(z)$ as follows:

$$\begin{cases} H_k(z) = a_k c_k H(zW^{(k+1/2)}) + a_k^* c_k^* H(zW^{-(k+1/2)}), \\ F_k(z) = a_k^* c_k H(zW^{(k+1/2)}) + a_k c_k^* H(zW^{-(k+1/2)}), \end{cases} \quad 0 \le k \le M-1 \tag{6}$$

where $a_k = e^{j\theta_k}, c_k = W^{(k+1/2)((N-1)/2)}$ and N is the length of $H(z)$. The impulse response coefficients $h_k(n)$ and $f_k(n)$ are given by

$$\begin{cases} h_k(n) = 2h(n)\cos\left((2k+1)\frac{\pi}{2M}\left(n-\frac{N-1}{2}\right)+\theta_k\right), \\ f_k(n) = 2h(n)\cos\left((2k+1)\frac{\pi}{2M}\left(n-\frac{N-1}{2}\right)-\theta_k\right), \end{cases} \quad \begin{cases} 0 \le n \le N-1 \\ 0 \le k \le M-1. \end{cases} \tag{7}$$

From (6) and (7), the analysis and synthesis filters are related as

$$\begin{cases} f_k(n) = h_k(N-1-n), \\ F_k(z) = z^{-(N-1)}\tilde{H}_k(z), \end{cases} \quad 0 \le k \le M-1. \tag{8}$$

3) θ_k are chosen such that

$$\theta_{k+1} = \theta_k \pm \frac{\pi}{2}, \qquad 0 \le k < M-1 \tag{9}$$

so that all the significant aliasing terms are cancelled. Furthermore, in order to ensure relatively flat overall magnitude distortion,

$$\theta_0 = \pm\left(\frac{\pi}{4} + l\frac{\pi}{2}\right) \text{ and } \theta_{M-1} = \pm\left(\frac{\pi}{4} + m\frac{\pi}{2}\right) \tag{10}$$

where l and m are arbitrary integers. Although other choices are possible, the following choice is used in this paper:

$$\theta_k = (-1)^k\frac{\pi}{4}, \qquad 0 \le k \le M-1. \tag{11}$$

This satisfies both (9) and (10).

4) The overall transfer function $T_0(z)$ is

$$T_0(z) = \frac{1}{M}\sum_{k=0}^{M-1} H_k(z)F_k(z) = \frac{z^{-(N-1)}}{M}\sum_{k=0}^{M-1} H_k(z)\tilde{H}_k(z). \tag{12}$$

Note that the above $T_0(z)$ has a linear phase independent of $H_k(z)$; therefore, the reconstructed signal has no phase distortion.

B. Spectral Factorization Approach to Pseudo-QMF Design [15]

Most of the material in this section can also be found in [15]. The main properties are summarized in the following:

1) The prototype filter $H(z)$ does not have linear-phase symmetry since it is obtained by spectral factorization. The length N is assumed to be a multiple of M, i.e., $N = mM$. No optimization procedure is needed. First, a $2M$th band filter $G'(z)$ is designed. Let ζ_2 be the stopband attenuation of $G'(z)$. From $G(z)$ by $G(z) = G'(z) + \zeta_2$. Find a spectral factor of $G(z)$ and set it to $H(z)$.

2) Let $b_k = e^{j\phi_k}$ and

$$S_k(z) \triangleq b_k H(zW^{(k+1/2)}) + b_k^* H(zW^{-(k+1/2)}); \tag{13}$$

then the analysis and synthesis filters $H_k(z)$ and $F_k(z)$ are obtained as follows:

$$H_k(z) = \begin{cases} S_k(z), & \text{even } k \\ z^{-(N-1)}\tilde{S}_k(z), & \text{odd } k \end{cases} \tag{14}$$

$$F_k(z) = z^{-(N-1)}\tilde{H}_k(z), \qquad 0 \le k \le M-1. \tag{15}$$

Note that the above choice for $F_k(z)$ is to ensure the linearity in the phase response of $T_0(z)$. The impulse response coefficients $h_k(n)$ and $f_k(n)$ are given by

$$h_k(n) = \begin{cases} s_k(n), & \text{even } k \\ s_k(N-1-n), & \text{odd } k \end{cases} \tag{16}$$

$$f_k(n) = h_k(N-1-n). \tag{17}$$

where $s_k(n) = 2h(n)\cos((2k+1)(\pi n/(2M) + \phi_k)$.

3) In order to ensure cancellation of the significant aliasing terms, ϕ_k should be satisfied:

$$\phi_{k+1} = \pm(2i+1)\frac{\pi}{2} - \phi_k, \qquad 0 \le k \le M-2 \tag{18}$$

where i is an integer. One of the choices that satisfies (18) is

$$\phi_k = \frac{\pi}{4} \qquad \forall k. \tag{19}$$

4) The overall transfer function $T_0(z)$ is

$$T_0(z) \simeq \frac{z^{-(N-1)}}{M} * c + \frac{z^{-(N-1)}}{M}[P_1(z) + P_2(z)] \tag{20}$$

where $P_j(z)$ cannot be eliminated for any choice of ϕ_k. The magnitude response of $P_1(z)$ is significant only in the region $|\omega| < \epsilon$, whereas that of $P_2(z)$ is significant only in the region $(\pi - \epsilon) < |\omega| < (\pi + \epsilon)$, where ϵ depends on the transition bandwidth of $H(z)$ and $0 < \epsilon < \pi/2M$. Consequently,

$$|T_0(e^{j\omega})| \simeq \text{constant}, \qquad \epsilon \le \omega \le (\pi - \epsilon). \tag{21}$$

$|T_0(e^{j\omega})|$ can have bumps or dips around $\omega = 0$ and $\omega = \pi$, depending on the values of $P_1(z)$ and $P_2(z)$.

C. Discussion Pertaining to the New Pseudo-QMF Design

The new pseudo-QMF design is a hybrid of the above pseudo-QMF designs. First, the prototype filter $H(z)$ is chosen to be a linear-phase filter. Moreover, $H(z)$ is designed such that it is a spectral factor of a $2M$th band filter. The analysis and synthesis filters $h_k(n)$ and $f_k(n)$ are cosine-modulated versions of the prototype filter $h(n)$ as in (7) with θ_k chosen as in (11). This choice of modulation yields an efficient implementation for the whole analysis/synthesis system. Together with the above $2M$th band constraint, it will be shown that $T_0(z) \simeq$ a delay. Even though $H(z)$ is a spectral factor of a $2M$th band filter, no spectral factorization is needed in the new approach. In other words, the $2M$th band constraints are imposed approximately. This approach yields NPR solutions where there is some aliasing at the reconstructed output (the level is comparable to the stopband attenuation). In order to obtain total aliasing cancellation (and thus, PR), not only should the prototype filter $h(n)$ be a spectral factor of a $2M$th band filter, but each polyphase component (in an M-phase decomposition) of $h(n)$ should be a spectral factor of a halfband filter [34].

III. The Novel Pseudo-QMF Bank

A. Properties of the New Pseudo-QMF Bank

Let $H(z) = \Sigma_{n=0}^{N-1} h(n)z^{-n}$ be the real-coefficient, linear-phase, even-length prototype filter of length N. Assume that $H(z)$ is a spectral factor of a $2M$th band filter $G(z)$, i.e.,

$$G(z) = z^{-(N-1)}H(z)\tilde{H}(z) = H^2(z) \tag{22}$$

in lieu of the linear-phase property of $H(z)$. The analysis and synthesis filters $h_k(n)$ and $f_k(n)$ are cosine-modulated versions of $h(n)$, i.e.,

$$\begin{cases} h_k(n)=2h(n)\cos\left((2k+1)\dfrac{\pi}{2M}\left(n-\dfrac{N-1}{2}\right)+(-1)^k\dfrac{\pi}{4}\right), \\ f_k(n)=2h(n)\cos\left((2k+1)\dfrac{\pi}{2M}\left(n-\dfrac{N-1}{2}\right)-(-1)^k\dfrac{\pi}{4}\right), \end{cases} \quad \begin{cases} 0 \le n \le N-1 \\ 0 \le k \le M-1. \end{cases} \tag{23}$$

Consequently, $H_k(z)$ and $F_k(z)$ are related as

$$\begin{cases} H_k(z) = a_k c_k H(zW^{(k+1/2)}) + a_k^* c_k^* H(zW^{-(k+1/2)}), \\ F_k(z) = z^{-(N-1)}\tilde{H}_k(z), \end{cases} \quad 0 \le k \le M-1 \tag{24}$$

where $a_k = e^{j\theta_k}, c_k = W^{(k+1/2)((N-1)/2)}$ and $\theta_k = (-1)^k(\pi/4)$. Note that the above filter choices are the same as those of the pseudo-QMF bank [20], with the exception that $H(z)$ here is a spectral factor of a $2M$th band filter. In the following section, it will be shown that $T_0(z) = (1/M)z^{-(N-1)}$.

B. The Overall Transfer Function $T_0(z)$

When the θ_k are chosen as in (11), the analysis/synthesis system is "approximately" alias-free, and the overall transfer function $T_0(z)$ can be expressed as

$$\frac{\hat{X}(z)}{X(z)} \simeq T_0(z) = \frac{z^{-(N-1)}}{M}\sum_{k=0}^{M-1} H_k(z)\tilde{H}_k(z). \tag{25}$$

Substituting (24) into (25), one obtains

$$\begin{aligned} z^{N-1}MT_0(z) &= \sum_{k=0}^{M-1}[a_k c_k H(zW^{(k+1/2)}) \\ &\quad + a_k^* c_k^* H(zW^{-(k+1/2)})] \\ &\quad \cdot [a_k^* c_k^* H(z^{-1}W^{-(k+1/2)}) + a_k c_k H(z^{-1}W^{(k+1/2)})] \\ &= \sum_{k=0}^{M-1}\{H(zW^{(k+1/2)})H(z^{-1}W^{-(k+1/2)}) \\ &\quad + H(zW^{-(k+1/2)})H(z^{-1}W^{(k+1/2)})\} \\ &\quad + \sum_{k=0}^{M-1}\{a_k^2 c_k^2 H(zW^{(k+1/2)})H(z^{-1}W^{(k+1/2)}) \\ &\quad + (a_k^2 c_k^2)^* H(zW^{-(k+1/2)})H(z^{-1}W^{-(k+1/2)})\} \\ &= \sum_{k=0}^{M-1}\{H(zW^{(k+1/2)})H(z^{-1}W^{-(k+1/2)}) \\ &\quad + H(zW^{(2M-k-1/2)})H(z^{-1}W^{-(2M-k-1/2)})\} \\ &\quad + \sum_{k=0}^{M-1}\{a_k^2 c_k^2 H(zW^{(k+1/2)})H(z^{-1}W^{(k+1/2)}) \\ &\quad + (a_k^2 c_k^2)^*[z^{-(N-1)}W^{(N-1)(k+1/2)}H(z^{-1}W^{(k+1/2)})] \\ &\quad \cdot [z^{N-1}W^{(N-1)(k+1/2)}H(zW^{(k+1/2)})]\} \end{aligned}$$

where the linear-phase property of $H(z)$ is used in the last summation of the above equation. After some simplification, one obtains

$$\begin{aligned} z^{N-1}MT_0(z) &= \sum_{k=0}^{2M-1} H(zW^{(k+1/2)})H(z^{-1}W^{-(k+1/2)}) \\ &\quad + \sum_{k=0}^{M-1} H(zW^{(k+1/2)})H(z^{-1}W^{(k+1/2)}) \\ &\quad \cdot [a_k^2 c_k^2 + (a_k^2 c_k^2)^* W^{(N-1)(2k+1)}]. \end{aligned} \tag{26}$$

Since

$$a_k^2 = W^{M(k+1/2)} \text{ and } c_k^2 = W^{(N-1)(k+1/2)},$$

after some simplification, the expression in the last summation is 0 for all k, i.e.,

$$[a_k^2 c_k^2 + (a_k^2 c_k^2)^* W^{(N-1)(2k+1)}] = 0 \qquad \forall k. \tag{27}$$

Substituting (27) into (26) yields

$$z^{N-1}MT_0(z) = \sum_{k=0}^{2M-1} H(zW^{(k+1/2)})H(z^{-1}W^{-(k+1/2)}). \tag{28}$$

Since $G(z) = z^{-(N-1)}H(z)H(z^{-1})$ is a $2M$th band filter, i.e.,

$$\sum_{k=0}^{2M-1} H(zW^k)H(z^{-1}W^{-k}) = 1, \tag{29}$$

the final result is

$$z^{N-1}MT_0(z) - 1, \text{ or equivalently, } T_0(z) = \frac{1}{M}z^{-(N-1)}. \tag{30}$$

In summary, as long as the prototype filter $H(z)$ is a linear-phase spectral factor of a $2M$th band filter and the $H_k(z)$ and $F_k(z)$ are obtained as in (24), then the overall distortion transfer function $T_0(z)$ is a delay. It remains to develop a design method to find a linear-phase filter $H(z)$ where $G(z) = H^2(z)$ is a $2M$th band filter. Furthermore, the method should produce a prototype filter $H(z)$ with high stopband attenuation. The next section focuses on the design method.

C. The Design Method (Even N)

In this section, we will describe the design method for the even N case, i.e., $N = 2(mM+m_1)$ where $0 \le m_1 \le M-1$. The odd N case will be considered in Section III-D. Defining $\boldsymbol{h}$ to be the vector consisting of the first $mM + m_1$ coefficients $h(n)$, i.e.,

$$\boldsymbol{h} = [h(0) \quad h(1) \quad \cdots \quad h(mM+m_1-1)]^t \tag{31}$$

and $\boldsymbol{e}(z)$ to be

$$\boldsymbol{e}(z) = [1 \quad z^{-1} \quad \cdots \quad z^{-(mM+m_1-1)}]^t, \tag{32}$$

then the prototype filter $H(z)$ can be represented as

$$H(z) = \boldsymbol{h}^t(\boldsymbol{I} \quad \boldsymbol{J})\begin{pmatrix} \boldsymbol{e}(z) \\ z^{-(mM+m_1)}\boldsymbol{e}(z)\end{pmatrix} \tag{33}$$

where the dimensions of both $\boldsymbol{I}$ and $\boldsymbol{J}$ are $(mM+m_1) \times (mM+m_1)$. Using the above notation, the $2M$th band filter $G(z)$ is

$$\begin{aligned} G(z) &= \sum_{n=0}^{4mM+4m_1-2} g(n)z^{-n} \\ &= H^2(z) = \boldsymbol{h}^t(\boldsymbol{I} \quad \boldsymbol{J})\begin{pmatrix} \boldsymbol{e}(z) \\ z^{-(mM+m_1)}\boldsymbol{e}(z)\end{pmatrix} \\ &\quad \cdot (\boldsymbol{e}^t(z) \quad z^{-(mM+m_1)}\boldsymbol{e}^t(z))\begin{pmatrix}\boldsymbol{I} \\ \boldsymbol{J}\end{pmatrix}\boldsymbol{h} \\ &= \boldsymbol{h}^t[\boldsymbol{U}(z) + z^{-(mM+m_1)}(\boldsymbol{J}\boldsymbol{U}(z) + \boldsymbol{U}(z)\boldsymbol{J}) \\ &\quad + z^{-2(mM+m_1)}\boldsymbol{J}\boldsymbol{U}(z)\boldsymbol{J}]\boldsymbol{h} \end{aligned} \tag{34}$$

where

$$\boldsymbol{U}(z) = \boldsymbol{e}(z)\boldsymbol{e}^t(z) = \begin{pmatrix} 1 \\ z^{-1} \\ \vdots \\ z^{-mM+m_1-1}\end{pmatrix} \cdot (1 \; z^{-1} \cdots z^{-(mM+m_1-1)}) = \sum_{n=0}^{2mM+2m_1-2} z^{-n}\boldsymbol{S}_n. \tag{35}$$

Note that the matrices $\boldsymbol{S}_n$ in (35) are constant matrices with elements 0 and 1. It can be verified that

$$[\boldsymbol{S}_n]_{k,l} = \begin{cases} 1, & k+l=n \\ 0, & \text{otherwise.}\end{cases} \tag{36}$$

Substituting (35) into (34), the following expression for $G(z)$ results:

$$\begin{aligned} G(z) &= \sum_{n=0}^{4mM+4m_1-2} g(n)z^{-n} \\ &= \boldsymbol{h}^t\Bigg[\sum_{n=0}^{2mM+2m_1-2} z^{-n}\boldsymbol{S}_n + z^{-(mM+m_1)} \\ &\quad \cdot \Bigg(\boldsymbol{J}\sum_{n=0}^{2mM+2m_1-2} z^{-n}\boldsymbol{S}_n \\ &\quad + \sum_{n=0}^{2mM+2m_1-2} z^{-n}\boldsymbol{S}_n\boldsymbol{J}\Bigg) \\ &\quad + z^{-(2mM+2m_1)}\boldsymbol{J}\sum_{n=0}^{2mM+2m_1-2} z^{-n}\boldsymbol{S}_n\boldsymbol{J}\Bigg]\boldsymbol{h} \\ &= \boldsymbol{h}^t\Bigg(\sum_{n=0}^{4mM+4m_1-2} z^{-n}\boldsymbol{D}_n\Bigg)\boldsymbol{h} \end{aligned} \tag{37}$$

where $\boldsymbol{D}_n$ depends on $\boldsymbol{S}_n$ and J as follows (see Appendix A for details):

$$\boldsymbol{D}_n = \begin{cases} \boldsymbol{S}_n; \\ \quad 0 \le n \le mM+m_1-1 \\ \boldsymbol{S}_n + \boldsymbol{J}\boldsymbol{S}_{n-mM-m_1} + \boldsymbol{S}_{n-mM-m_1}\boldsymbol{J}; \\ \quad mM+m_1 \le n \le 2(mM+m_1-1) \\ \boldsymbol{J}\boldsymbol{S}_{mM+m_1-1} + \boldsymbol{S}_{mM+m_1-1}\boldsymbol{J}; \\ \quad n = 2(mM+m_1)-1 \\ \boldsymbol{J}\boldsymbol{S}_{n-mM-m_1} + \boldsymbol{S}_{n-mM-m_1}\boldsymbol{J} + \boldsymbol{J}\boldsymbol{S}_{n-2mM-2m_1}\boldsymbol{J}; \\ \quad 2(mM+m_1) \le n \le 3(mM+m_1)-2 \\ \boldsymbol{J}\boldsymbol{S}_{n-2mM-2m_1}\boldsymbol{J}; \\ \quad 3(mM+m_1)-1 \le n \le 4(mM+m_1)-2. \end{cases} \tag{38}$$

The objective is to find $\boldsymbol{h}$ such that $G(z)$ is a $2M$th band filter, i.e., see (39), which is at the bottom of this page: Equating

$$g_n = \begin{cases} 0; & n = 2(mM+m_1) - 1 - 2lM, \begin{cases} 1 \le l \le m-1, & m_1 = 0 \\ 1 \le l \le m, & m_1 \ne 0 \end{cases} \\ \dfrac{1}{2M}; & n = 2(mM+m_1)-1. \end{cases} \tag{39}$$

the terms with the same power of z^{-1} in (37) and using (38) and (39), the following m constraints on $\boldsymbol{h}$ are obtained:

$$\begin{cases} \boldsymbol{h}^t \boldsymbol{S}_n \boldsymbol{h} = 0; \\ \quad \begin{cases} \left\lfloor \frac{(m+1)}{2} \right\rfloor \le l \le (m-1), & m_1 = 0 \\ \left\lfloor \frac{(m+1)}{2} \right\rfloor \le l \le m, & m_1 \ne 0 \end{cases} \\ \boldsymbol{h}^t(\boldsymbol{S}_n + \boldsymbol{J}\boldsymbol{S}_{n-mM-m_1} + \boldsymbol{S}_{n-mM-m_1}\boldsymbol{J})\boldsymbol{h} = 0; \\ \quad 1 \le l \le \left\lfloor \frac{(m+1)}{2} \right\rfloor - 1 \\ \boldsymbol{h}^t(\boldsymbol{J}\boldsymbol{S}_{mM+m_1-1} + \boldsymbol{S}_{mM+m_1-1}\boldsymbol{J})\boldsymbol{h} = \frac{1}{2M} \end{cases} \tag{40}$$

In summary, given m, m_1, and M, one can calculate $\boldsymbol{S}_n$ as in (36). The $2M$th band constraint on $G(z)$ becomes the constraints on $\boldsymbol{h}$ as shown in (40) and (51) for even and odd N, respectively. Suppose that one is able to obtain $\boldsymbol{h}$ such that it satisfies the constraints in (40) and (51); then the resulting prototype filter $H(z)$ [found using (33) or (46)] is the spectral factor of the $2M$th band filter $G(z)$. Moreover, the linear-phase property of $H(z)$ is structurally imposed on the problem. Thus, the above design method finds a spectral factor of a $2M$th band filter without taking the spectral factor! As long as the filter coefficients $h(n)$ satisfy the $2M$th band constraints in (40) and (51), then there is no amplitude or phase distortion at the output. The only reconstruction error is aliasing, which can be minimized by finding solutions with high stopband attenuation.

Besides the above m constraints, $\boldsymbol{h}$ should also yield a prototype filter with good stopband attenuation, i.e., h should minimize

$$\int_{\omega_S}^{\pi} |H(e^{j\omega})|^2 \, d\omega \tag{41}$$

and satisfy (30). The eigenfilter method [26], [27] represents the above integral as a quadratic form (see Appendix B for the details):

$$\int_{\omega_S}^{\pi} |H(e^{j\omega})|^2 \, d\omega = \boldsymbol{h}^t \boldsymbol{P} \boldsymbol{h}. \tag{42}$$

Thus, the design problem can be stated as follows:

$$\text{find } \boldsymbol{h} \text{ that minimizes } \boldsymbol{h}^t\boldsymbol{P}\boldsymbol{h} \text{ and satisfies (40) where} \tag{43}$$

$$[\boldsymbol{P}]_{k,l} = 2\sum_{i=1}^{K} \beta_i \int_{\omega_{i,1}}^{\omega_{i,2}} [\cos\omega(k-l) + \cos\omega(N-1-k-l)] d\omega, \quad 0 \le k, l \le mM + m_1 - 1. \tag{44}$$

Here, K is the number of stopbands of $H(e^{j\omega}), \beta_i$ are their relative weights, and $\omega_{i,1}$ and $\omega_{i,2}$ are the bandedges of these stopbands.

The above optimization problem can be solved very accurately by the nonlinearity constrained minimization algorithm of Schittkowski [28]–[29]. This minimization algorithm is coded in the IMSL Math library [30] under subroutine DNCONG. The DNCONG subroutine is used to generate all examples in this paper.

D. The Design Method (Odd N)

In this section, we will describe the design method for the odd N case, i.e., $N = 2(mM + m_1) + 1$ where $0 \le m_1 \le M-1$. Except for some modifications, the formulations in this section are very similar to those in Section III-C. Defining $\boldsymbol{h}$ and $\boldsymbol{e}(z)$ as follows,

$$\begin{cases} \boldsymbol{h} = [h(0) \quad h(1) \quad \cdots \quad h(mM+m_1)]^t \\ \boldsymbol{e}(z) = [1 \quad z^{-1} \quad \cdots \quad z^{-(mM+m_1)}]^t, \end{cases} \tag{45}$$

then the prototype filter $H(z)$ can be represented as

$$H(z) = \boldsymbol{h}^t \boldsymbol{V} (\boldsymbol{I} \quad \boldsymbol{J}) \begin{pmatrix} \boldsymbol{e}(z) \\ z^{-(mM+m_1)}\boldsymbol{e}(z) \end{pmatrix} \tag{46}$$

where the dimensions of both $\boldsymbol{I}$ and $\boldsymbol{J}$ are $(mM + m_1 + 1) \times (mM + m_1 + 1)$. Using the above notation, the corresponding $2M$th band filter $G(z)$ is

$$\begin{aligned} G(z) &= \sum_{n=0}^{4mM+4m_1} g(n) z^{-n} \\ &= H^2(z) = \boldsymbol{h}^t \boldsymbol{V}(\boldsymbol{I} \quad \boldsymbol{J}) \begin{pmatrix} \boldsymbol{e}(z) \\ z^{-(mM+m_1)}\boldsymbol{e}(z) \end{pmatrix} \\ &\quad \cdot (\boldsymbol{e}^t(z) \quad z^{-(mM+m_1)}\boldsymbol{e}^t(z)) \begin{pmatrix} \boldsymbol{I} \\ \boldsymbol{J} \end{pmatrix} \boldsymbol{V}\boldsymbol{h} \\ &= \boldsymbol{h}^t \boldsymbol{V}[\boldsymbol{U}(z) + z^{-(mM+m_1)}(\boldsymbol{J}\boldsymbol{U}(z) + \boldsymbol{U}(z)\boldsymbol{J}) \\ &\quad + z^{-2(mM+m_1)}\boldsymbol{J}\boldsymbol{U}(z)\boldsymbol{J}]\boldsymbol{V}\boldsymbol{h} \end{aligned} \tag{47}$$

where $\boldsymbol{U}(z)$ is as in (35). Consequently, as similar to Section III-C, $G(z)$ can be expressed as follows:

$$G(z) = \sum_{n=0}^{4mM+4m_1} g(n) z^{-n} = \boldsymbol{h}^t \boldsymbol{V} \left(\sum_{n=0}^{4mM+4m_1} z^{-n} \boldsymbol{D}_n \right) \boldsymbol{V}\boldsymbol{h} \tag{48}$$

where $\boldsymbol{D}_n$ depends on $\boldsymbol{S}_n$ and J as follows (see Appendix A for details):

$$\boldsymbol{D}_n = \begin{cases} \boldsymbol{V}\boldsymbol{S}_n\boldsymbol{V}; \\ \quad 0 \le n \le mM + m_1 - 1 \\ \boldsymbol{V}(\boldsymbol{S}_n + \boldsymbol{J}\boldsymbol{S}_{n-mM-m_1} + \boldsymbol{S}_{n-mM-m_1}\boldsymbol{J})\boldsymbol{V}; \\ \quad mM + m_1 \le n \le 2(mM + m_1) - 1 \\ \boldsymbol{V}(\boldsymbol{S}_{2mM+2m_1} + \boldsymbol{J}\boldsymbol{S}_{mM+m_1} + \boldsymbol{S}_{mM+m_1}\boldsymbol{J} + \boldsymbol{J}\boldsymbol{S}_0\boldsymbol{J})\boldsymbol{V}; \\ \quad n = 2(mM + m_1) \\ \boldsymbol{V}(\boldsymbol{J}\boldsymbol{S}_{n-mM-m_1} + \boldsymbol{S}_{n-mM-m_1}\boldsymbol{J} + \boldsymbol{J}\boldsymbol{S}_{n-2mM-2m_1}\boldsymbol{J})\boldsymbol{V}; \\ \quad 2(mM + m_1) + 1 \le n \le 3(mM + m_1) \\ \boldsymbol{V}\boldsymbol{J}\boldsymbol{S}_{n-2mM-2m_1}\boldsymbol{J}\boldsymbol{V}; \\ \quad 3(mM + m_1) + 1 \le n \le 4(mM + m_1). \end{cases} \tag{49}$$

The objective is to find $\boldsymbol{h}$ such that $G(z)$ is a $2M$th band filter, i.e.,

$$g_n = \begin{cases} 0; & n = 2(mM + m_1) - 2lM, \quad 1 \le l \le m \\ \frac{1}{2M}; & n = 2(mM + m_1). \end{cases} \tag{50}$$

Equating the terms with the same power of z^{-1} in (48) and using (49) and (50), the following m constraints on $\boldsymbol{h}$ are

$$\begin{cases} \boldsymbol{h}^t \boldsymbol{V}\boldsymbol{S}_n \boldsymbol{V}\boldsymbol{h} = 0; \\ \quad \left\lfloor \frac{m}{2} + 1 \right\rfloor \le l \le m \\ \boldsymbol{h}^t \boldsymbol{V}(\boldsymbol{S}_n + \boldsymbol{J}\boldsymbol{S}_{n-mM-m_1} + \boldsymbol{S}_{n-mM-m_1}\boldsymbol{J})\boldsymbol{V}\boldsymbol{h} = 0; \\ \quad 1 \le l \le \left\lfloor \frac{m}{2} \right\rfloor \\ \boldsymbol{h}^t (\boldsymbol{S}_{2mM+2m_1} + \boldsymbol{J}\boldsymbol{S}_{mM+m_1} + \boldsymbol{S}_{mM+m_1}\boldsymbol{J} + \boldsymbol{J}\boldsymbol{S}_0\boldsymbol{J})\boldsymbol{V}\boldsymbol{h} = \frac{1}{2M} \end{cases} \tag{51}$$

where $n = 2M(m - l) + 2m_1$.

Similar to the quadratic constraints (40) in Section III-C, the conditions in (51) are another form of the $2M$th band constraint on $G(z)$. Using the similar eigenfilter formulation, the design problem for the odd N case can be stated as follows:

$$\text{find } \boldsymbol{h} \text{ that minimizes } \boldsymbol{h}^t \boldsymbol{P}\boldsymbol{h} \text{ and satisfies (51) where} \tag{52}$$

$$[\boldsymbol{P}]_{k,l} = 2\sum_{i=1}^{K} \beta_i \int_{\omega_{i,1}}^{\omega_{i,2}} [\cos\omega(k-l) + \cos\omega(N-1-k-l)]\, d\omega, \quad 0 \le k, l \le mM + m_1. \tag{53}$$

Here, K is the number of stopbands of $H(e^{j\omega})$. β_i are their relative weights, and $\omega_{i,1}$ and $\omega_{i,2}$ are the band-edges of these stopbands. The design procedure is as follows.

Design Procedure for the Novel Pseudo-QMF Bank:

1) Given m, m_1, M, and ω_S, compute $N = 2(mM + m_1)$ or $N = 2(mM + m_1) + 1$, depending on the choice of N (even or odd), $\boldsymbol{S}_n$ as in (36), and $\boldsymbol{P}$ as in (44) or (53).
2) Design an initialization low-pass filter $\hat{H}(z)$ approximating the frequency response in Fig. 1(c) using any filter design algorithm. The eigenfilter method [26] is used in this paper. From $\boldsymbol{h}$ as in (31) or (45) from the impulse coefficient of $\hat{H}(z)$.
3) Compute the quadratic conditions (40) or (51) and their gradients (to be used in DNCONG). Compute the stopband error $\boldsymbol{h}^t\boldsymbol{P}\boldsymbol{h}$ and its gradient.
4) Call subroutine DNCONG to solve the quadratic-constrained minimization problem in (43) or (52).
5) From the output of DNCONG, find $h_k(n)$ and $f_k(n)$ as in (23). $H_k(z)$ and $F_k(z)$ are the analysis and synthesis filters of the novel pseudo-QMF bank. The overall distortion function $T_0(z)$ is a delay, and the aliasing level is the same as the stopband attenuation of $H(z)$.

Comments on the Design Procedure:

1) The nonlinear constrained minimization algorithm by Schittkowski [28], [29] finds a solution vector $\boldsymbol{h}$ that satisfies the m constraints in (40) or (51) up to a small prescribed positive number η, i.e.,

$$\begin{cases} |\boldsymbol{h}^t \boldsymbol{S}_n \boldsymbol{h}| \le \eta; \\ \quad \left\lfloor \frac{m}{2} \right\rfloor \le l \le (m-1) \\ |\boldsymbol{h}^t (\boldsymbol{S}_n + \boldsymbol{J}\boldsymbol{S}_{n-mM} + \boldsymbol{S}_{n-mM}\boldsymbol{J})\boldsymbol{h}| \le \eta; \\ \quad 1 \le l \le \left\lfloor \frac{m}{2} \right\rfloor - 1 \\ |\boldsymbol{h}^t (\boldsymbol{J}\boldsymbol{S}_{mM-1} + \boldsymbol{S}_{mM-1}\boldsymbol{J})\boldsymbol{h} - \frac{1}{2M}| \le \eta \end{cases} \tag{54}$$

for the even N case. Consequently, for smaller η, the $2M$th band condition is satisfied more closely, and δ_1 is smaller. Typically, $\eta \le 1 \times 10^{-13}$ in the design method.
2) The constraints in (40) or (51) are quadratic in $\boldsymbol{h}$; therefore their gradients (to be used in the optimization algorithm) are easy to compute. Even though the stopband error of $H(e^{j\omega})$ can take many forms such as least squares (41) or minimax [32], the least-squares representation is used since its gradient is simple to compute.

IV. Examples

Example 1: In this example, a four-channel pseudo-QMF bank is designed using the above method. Let $m = 14, m_1 = 0, M = 4, K = 1, \beta_1 = 1, \omega_{1,1} = 0.23\pi, \omega_{1,2} = \pi$, and $\eta = 1 \times 10^{-13}$. The length of $H(z)$ is chosen to be $N = 112$. $\boldsymbol{P}$ is computed using numerical integration with 400 grid points. The magnitude responses of the optimized prototype filter $H(z)$, the corresponding analysis filters $H_k(z)$, the overall distortion transfer function $T_0(z)$, and the aliasing transfer function $t_l(z), 1 \le l \le M-1$ are plotted in Fig. 2(a)–(d), respectively. Note that the stopband attenuation of $H(z)$ and $H_k(z)$ is about -107 dB. Consequently, as shown in Fig. 2(d), the aliasing level is also about -107 dB. The magnitude response of $T_0(z)$ is plotted in Fig. 2(c) on an expanded logarithmic scale. Here, $\delta_1 \le 3.35 \times 10^{-11}$ dB, which is very small in normal scale. The above four-channel pseudo-QMF bank was also simulated. The spectrum of the input signal and the reconstructed error are plotted in Fig. 2(e) and (f), respectively. In agreement with the theory, the output signal $\hat{x}(n)$ approximates $x(n)$ with -107 dB error.

Example 2: In this example, a 16-channel pseudo-QMF bank is designed using the above method. Let $m = 12, m_1 = 0, M = 16, K = 2, \beta_1 = 1.2, \beta_2 = 1.0, \omega_{1,1} = 0.059\pi, \omega_{1,2} = 0.43\pi, \omega_{2,1} = 0.43\pi, \omega_{2,2} = \pi$, and $\eta = 1 \times 10^{-13}$. The length of $H(z)$ is chosen to be $N = 384$. $\boldsymbol{P}$ is computed using numerical integration with 400 grid points.

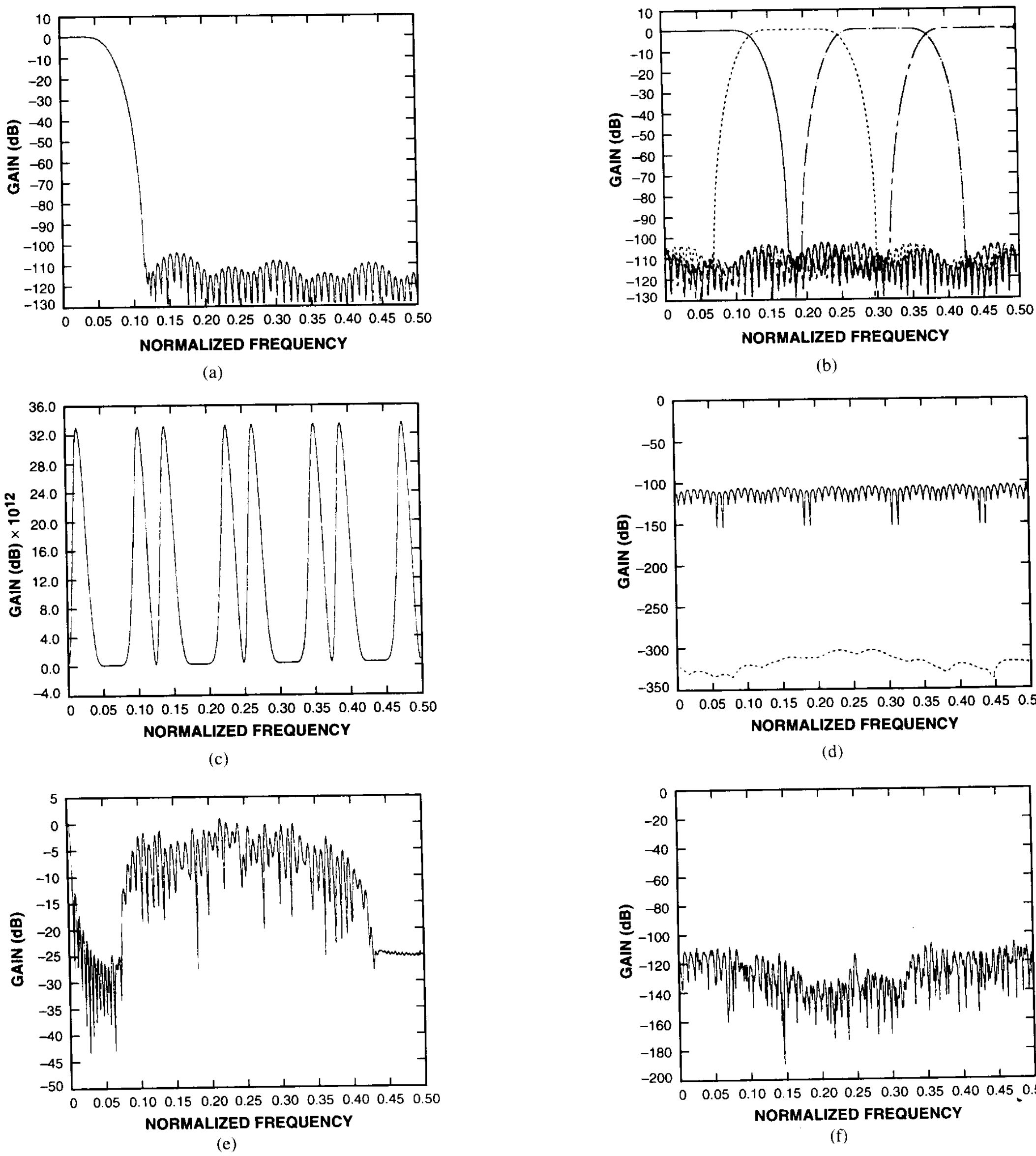

Fig. 2. Example 1. Magnitude response of the optimized prototype filter $H(z)$; (b) magnitude response plots for the analysis filters $H_k(z)$; (c) magnitude response plot for the overall distortion $T_0(z)$; (d) magnitude response plots for the alias transfer functions $T_k(z)$; (e) spectrum of the input signal; (f) reconstruction error.

The magnitude responses of the optimized prototype filter $H(z)$, the corresponding analysis filters $H_k(z)$, the overall distortion transfer function $T_0(z)$, and the aliasing transfer functions $T_l(z), 1 \leq l < M-1$ are plotted in Fig. 3(a)–(d), respectively. Note that the stopband attenuation of $H(z)$ and $H_k(z)$ is about -100 dB, except at the bandedges. Consequently, as shown in Fig. 3(d), the aliasing level is also about -95 dB. The magnitude response of $T_0(z)$ is plotted in Fig. 3(c) on an expanded logarithmic scale. Here, $\delta_1 \leq 1.8 \times 10^{-13}$ dB, which is very small in normal scale. The above 16-channel pseudo-QMF bank is simulated with the same input signal as in Example 1. The spectrum of reconstructed error is plotted in Fig. 3(e). Here, the signal $\hat{x}(n)$ approximates $x(n)$ with -95 dB error.

V. Conclusion

A new algorithm to design a pseudo-QMF bank is presented. The prototype filter is a linear-phase spectral factor of a $2M$th band filter. The analysis and synthesis filters are cosine-modulated versions of the prototype filter. As a result, the overall transfer function $T_0(z)$ is a delay, and the alias level is comparable to the stopband attenuation of the prototype filter.

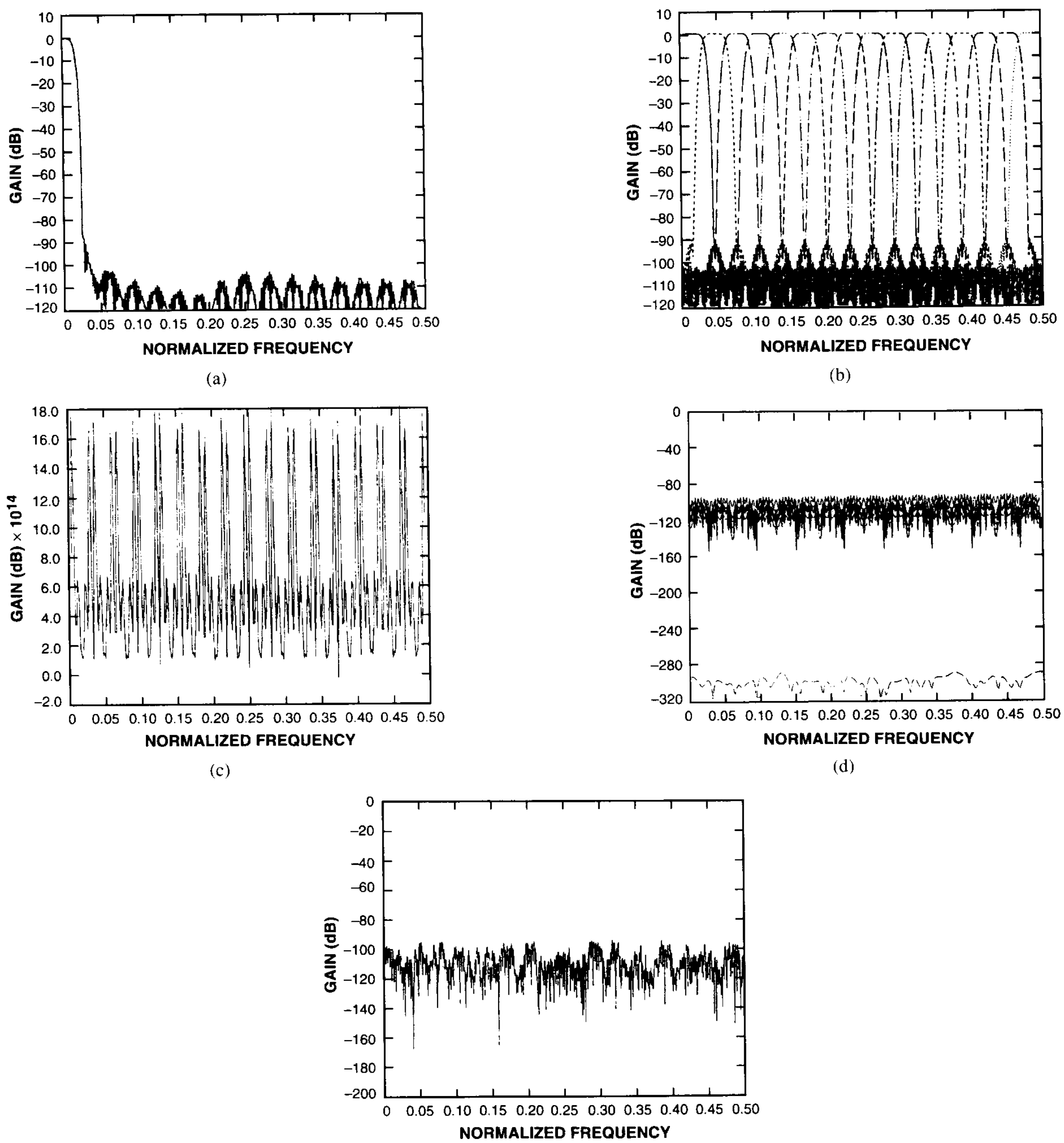

Fig. 3. (a) Example 2. Magnitude response of the optimized prototype filter $H(z)$; (b) magnitude response plots for the analysis filters $H_k(z)$; (c) magnitude response plot for the overall distortion $T_0(z)$; (d) magnitude response plots for the alias transfer functions $T_k(k)$; (e) reconstruction error.

A method to find the linear-phase spectral factor of a $2M$th band filter without taking the spectral factor is also described. This method relates the $2M$th band condition to a set of m quadratic constraints in $\boldsymbol{h}$, the impulse coefficients of $H(z)$. These m quadratic constraints are minimized together with the stopband error of $H(z)$, and yield a prototype filter with -100 dB attenuation. Moreover, the m quadratic constraints are satisfied with error $\eta \leq 1 \times 10^{-13}$.

Two pseudo-QMF banks were designed using this novel algorithm. The reconstruction error of the four-channel pseudo-QMF banks was about -107 dB whereas the stopband attenuation of the analysis and synthesis filters was also about -107 dB. The second design example concerned a 16-channel pseudo-QMF bank. The resulting reconstruction error was -95 dB, while the stopband attenuation of the analysis and synthesis filters were also about -95 dB. Both pseudo-QMF banks were simulated with the same input. In agreement with the theory, the reconstruction errors were -107 and -95 dB, respectively, for the four-channel and 16-channel pseudo-QMF banks.

Appendix A

In this Appendix, the relation among $\boldsymbol{D}_n, \boldsymbol{S}_n$, and J is derived.

- *Even* $N\,(N = 2(mM + m_1))$

From Section III-C and (36),

$$
\begin{aligned}
G(z) &= \sum_{n=0}^{4mM+4m_1-2} g(n)z^{-n} \\
&= \boldsymbol{h}^t \Bigg[\sum_{n=0}^{2mM+2m_1-2} z^{-n}\boldsymbol{S}_n + z^{-(mM+m_1)} \\
&\quad \cdot \left(\boldsymbol{J} \sum_{n=0}^{2mM+2m_1-2} z^{-n}\boldsymbol{S}_n + \sum_{n=0}^{2mM+2m_1-2} \cdot z^{-n}\boldsymbol{S}_n\boldsymbol{J} \right) \\
&\quad + z^{-2(mM+m_1)}\boldsymbol{J} \sum_{n=0}^{2mM+2m_1-2} z^{-n}\boldsymbol{S}_n\boldsymbol{J} \Bigg] \boldsymbol{h} \\
&= \boldsymbol{h}^t \left(\sum_{n=0}^{4mM-2} z^{-n}\boldsymbol{D}_n \right) \boldsymbol{h}
\end{aligned}
\tag{A.1}
$$

Grouping the like powers of z^{-1}, (A.1) becomes

$$
\begin{aligned}
G(z) = \boldsymbol{h}^t \Bigg\{ & \sum_{n=0}^{mM+m_1-1} z^{-n}\boldsymbol{S}_n + \sum_{n=mM+m_1}^{2mM+2m_1-2} \\
& \cdot z^{-n}(\boldsymbol{S}_n + \boldsymbol{J}\boldsymbol{S}_{n-mM-m_1} + \boldsymbol{S}_{n-mM-m_1}\boldsymbol{J}) \\
& + z^{-(2mM+2m_1-1)}(\boldsymbol{J}\boldsymbol{S}_{mM+m_1-1} + \boldsymbol{S}_{mM+m_1-1}\boldsymbol{J}) \\
& + \sum_{n=2mM+2m_1}^{3mM+3m_1-2} z^{-n}(\boldsymbol{J}\boldsymbol{S}_{n-mM-m_1} + \boldsymbol{S}_{n-mM-m_1}\boldsymbol{J} \\
& + \boldsymbol{J}\boldsymbol{S}_{n-2mM-2m_1}\boldsymbol{J}) \\
& + \sum_{n=3mM+3m_1-1}^{4mM+4m_1-2} z^{-n}\boldsymbol{J}\boldsymbol{S}_{n-2mM-2m_1}\boldsymbol{J} \Bigg\} \boldsymbol{h}.
\end{aligned}
\tag{A.2}
$$

From the above two equations, $\boldsymbol{D}_n$ is as shown in n (38).

- *Odd* $N\,(N = 2(mM + m_1) + 1)$

From Section III-D and (46)

$$
\begin{aligned}
G(z) &= \sum_{n=0}^{4mM+4m_1} g(n)z^{-n} \\
&= \boldsymbol{h}^t\boldsymbol{V} \Bigg[\sum_{n=0}^{2mM+2m_1} z^{-n}\boldsymbol{S}_n + z^{-(mM+m_1)} \\
&\quad \cdot \left(\boldsymbol{J} \sum_{n=0}^{2mM+2m_1} z^{-n}\boldsymbol{S}_n + \sum_{n=0}^{2mM+2m_1} z^{-n}\boldsymbol{S}_n\boldsymbol{J} \right) \\
&\quad + z^{-2(mM+m_1)}\boldsymbol{J} \sum_{n=0}^{2mM+2m_1} z^{-n}\boldsymbol{S}_n\boldsymbol{J} \Bigg] \boldsymbol{V}\boldsymbol{h} \\
&= \boldsymbol{h}^t\boldsymbol{V} \left(\sum_{n=0}^{4mM+4m_1} z^{-n}\boldsymbol{D}_n \right) \boldsymbol{V}\boldsymbol{h}.
\end{aligned}
\tag{A.3}
$$

Grouping the like powers of z^{-1}, (A.3) becomes

$$
\begin{aligned}
G(z) = \boldsymbol{h}^t\boldsymbol{V} \Bigg\{ & \sum_{n=0}^{mM+m_1-1} z^{-n}\boldsymbol{S}_n + \sum_{n=mM+m_1}^{2(mM+m_1)-1} \\
& \cdot z^{-n}(\boldsymbol{S}_n + \boldsymbol{J}\boldsymbol{S}_{n-mM-m_1} + \boldsymbol{S}_{n-mM-m_1}\boldsymbol{J}) \\
& + z^{-2(mM_2m_1)}(\boldsymbol{S}_{2mM+2m_1} + \boldsymbol{J}\boldsymbol{S}_{mM+m_1} \\
& + \boldsymbol{S}_{mM+m_1}\boldsymbol{J} + \boldsymbol{J}\boldsymbol{S}_0\boldsymbol{J}) \\
& + \sum_{n=2(mM+m_1)+1}^{3(mM+m_1)} z^{-n}(\boldsymbol{J}\boldsymbol{S}_{n-mM-m_1} \\
& + \boldsymbol{S}_{n-mM-m_1}\boldsymbol{J} + \boldsymbol{J}\boldsymbol{S}_{n-2mM-2m_1}\boldsymbol{J}) \\
& + \sum_{n=3(mM+m_1)+1}^{4(mM+m_1)} z^{-n}\boldsymbol{J}\boldsymbol{S}_{n-2mM-2m_1}\boldsymbol{J} \Bigg\} \boldsymbol{V}\boldsymbol{h}.
\end{aligned}
\tag{A.4}
$$

From the above two equations, $\boldsymbol{D}_n$ is as shown in (49).

Appendix B

The stopband error of $H(z)$ is defined to be

$$
\begin{aligned}
e_S &= \sum_{i=1}^{K} \beta_i \int_{\omega_{i,1}}^{\omega_{i,2}} |H(e^{j\omega})|^2\, d\omega \\
&= \sum_{i=1}^{K} \beta_i \int_{\omega_{i,1}}^{\omega_{i,2}} H(e^{j\omega})H^*(e^{j\omega})\, d\omega
\end{aligned}
\tag{B.1}
$$

where K is the number of stopbands, β_i are their relative weighting, and $\omega_{i,1}$ and $\omega_{i,2}$ are the bandedges of these stopbands. We will express e_S in a quadratic form below.

- *Even* N

Using the notation in (33) for $H(z)$, e_S becomes

$$
\begin{aligned}
e_S = \boldsymbol{h}^t \sum_{i=1}^{K} \beta_i \int_{\omega_{i,1}}^{\omega_{i,2}} & (\boldsymbol{I} \quad \boldsymbol{J}) \begin{pmatrix} \boldsymbol{e}(e^{j\omega}) \\ e^{-j(mM+m_1)\omega}\boldsymbol{e}(e^{j\omega}) \end{pmatrix} \\
& \cdot (\tilde{\boldsymbol{e}}(e^{j\omega}) \quad e^{j(mM+m_1)\omega}\tilde{\boldsymbol{e}}(e^{j\omega})) \begin{pmatrix} \boldsymbol{I} \\ \boldsymbol{J} \end{pmatrix} d\omega\boldsymbol{h}.
\end{aligned}
\tag{B.2}
$$

Simplifying the above expression,

$$
\begin{aligned}
e_S = \boldsymbol{h}^t \sum_{i=1}^{K} \beta_i \int_{\omega_{i,1}}^{\omega_{i,2}} & (\boldsymbol{e}(e^{j\omega})\tilde{\boldsymbol{e}}(e^{j\omega}) \\
& + e^{-j(mM+m_1)\omega}\boldsymbol{J}\boldsymbol{e}(e^{j\omega})\tilde{\boldsymbol{e}}(e^{j\omega}) \\
& + e^{j(mM+m_1)\omega}\boldsymbol{e}(e^{j\omega})\tilde{\boldsymbol{e}}(e^{j\omega})\boldsymbol{J} \\
& + \boldsymbol{J}\boldsymbol{e}(e^{j\omega})\tilde{\boldsymbol{e}}(e^{j\omega})\boldsymbol{J})\, d\omega\boldsymbol{h}.
\end{aligned}
\tag{B.3}
$$

The matrix $\boldsymbol{P}$ can be extracted from the above equation, i.e.,

$$
\begin{aligned}
\boldsymbol{P} = \sum_{i=1}^{K} \beta_i \int_{\omega_{i,1}}^{\omega_{i,2}} & (\boldsymbol{e}(e^{j\omega})\tilde{\boldsymbol{e}}(e^{j\omega}) \\
& + e^{-j(mM+m_1)\omega}\boldsymbol{J}\boldsymbol{e}(e^{j\omega})\tilde{\boldsymbol{e}}(e^{j\omega}) \\
& + e^{j(mM+m_1)\omega}\boldsymbol{e}(e^{j\omega})\tilde{\boldsymbol{e}}(e^{j\omega})\boldsymbol{J} \\
& + \boldsymbol{J}\boldsymbol{e}(e^{j\omega})\tilde{e}(e^{j\omega})\boldsymbol{J})\, d\omega.
\end{aligned}
\tag{B.4}
$$

This matrix $\boldsymbol{P}$ is a real, symmetric, and positive definite matrix. Its elements are

$$[\boldsymbol{P}]_{k,l} = 2\sum_{i=1}^{K} \beta_i \int_{\omega_{i,1}}^{\omega_2} [\cos\omega(k-l) + \cos\omega(N-1-k-l)]\, d\omega, \quad 0 \le k,l \le mM + m_1 - 1. \tag{B.5}$$

Thus, given N and ω_S, one can compute $\boldsymbol{P}$ from the above expression. In the example, $\boldsymbol{P}$ was evaluated using numerical integration with 400 grid points.

- *Odd N*

Using the notation in (46) for $H(z), e_S$ becomes

$$e_S = \boldsymbol{h}^t \boldsymbol{V} \sum_{i=1}^{K} \beta_i \int_{\omega_{i,1}}^{\omega_{i,2}} (\boldsymbol{I} \quad \boldsymbol{J}) \begin{pmatrix} \boldsymbol{e}(e^{j\omega}) \\ e^{-j(mM+m_1)\omega} \boldsymbol{e}(e^{j\omega}) \end{pmatrix} \cdot \left(\tilde{\mathbf{e}}(e^{j\omega}) \quad e^{j(mM+m_1)\omega} \tilde{\mathbf{e}}(e^{j\omega})\right) \begin{pmatrix} \boldsymbol{I} \\ \boldsymbol{J} \end{pmatrix} d\omega \boldsymbol{V}\boldsymbol{h}. \tag{B.6}$$

Simplifying the above expression similarly to the above odd case, we obtain

$$e_S = \boldsymbol{h}^t \boldsymbol{P} \boldsymbol{h}$$

where

$$[\boldsymbol{P}]_{k,l} = 2\nu \sum_{i=1}^{K} \beta_i \int_{\omega_{i,1}}^{\omega_2} [\cos\omega(k-l) + \cos\omega(N-1-k-l)]\, d\omega, \quad 0 \le k,l \le mM + m_1 \tag{B.7}$$

and

$$\nu = \begin{cases} 1, & 0 \le k,l \le mM + m_1 - 1 \\ \frac{1}{2}, & k = mM + m_1, 0 \le l \le mM + m_1 - 1 \\ \frac{1}{2}, & l = mM + m_1, 0 \le k \le mM + m_1 - 1 \\ \frac{1}{4}, & k = l = mM + m_1. \end{cases} \tag{B.8}$$

Thus, given N and ω_S, one can compute $\boldsymbol{P}$ from the above expression.

REFERENCES

[1] D. Esteban and C. Galand, "Application of quadrature mirror filters to split-band voice coding schemes," in *Proc. IEEE Int. Conf. ASSP* (Hartford, CT), May 1977, pp. 191–195.

[2] R. E. Crochiere and L. R. Rabiner, *Multirate Signal Processing*. Englewood Cliffs, NJ: Prentice-Hall, 1983.

[3] T. P. Barnwell, III, "Subband coder design incorporating recursive quadrature filters and optimum ADPCM coders," *IEEE Trans. Acoust. Speech Signal Processing*, vol. ASSP-30, pp. 751–765, Oct. 1982.

[4] R. V. Cox, D. E. Boch, K. B. Bauer, J. D. Johnston, and J. H. Snyder, "The analog voice privacy system," in *Proc. IEEE Int. Conf. ASSP*, Apr. 1986, pp. 341–344.

[5] J. W. Woods and S. P. O'Neil, "Subband coding of images," *IEEE Trans. Acoust. Speech Signal Processing*, vol. ASSP-34, pp. 1278–1288, Oct. 1986.

[6] C. S. Kim, J. Bruder, M. J. T. Smith, and R. M. Mersereau, "Subband coding of color images using finite state vector quantization," in *Proc. IEEE Int. Conf. ASSP*, Apr. 1988, pp. 753–756.

[7] J. Kovacevic, D. J. Le Gall, and M. Vetterli, "Image coding with windowed modulated filter banks," in *Proc. IEEE Int. Conf. ASSP*, May 1989, pp. 1949–1952.

[8] M. J. Smith and T. P. Barnwell, III, "Exact reconstruction techniques for tree-structured subband coders," *IEEE Trans. Acoust. Speech Signal Processing*, vol. ASSP-34, pp. 434–441, June 1986.

[9] F. Mintzer, "Filters for distortion-free two-band multirate filter banks," *IEEE Trans. Acoust. Speech Signal Processing*, pp. 626–630, June 1985.

[10] P. P. Vaidyanathan, "Theory and design of M-channel maximally decimated quadrature mirror filters with arbitrary M, having perfect reconstruction property," *IEEE Trans. Acoust. Speech Signal Processing*, vol. ASSP-35, pp. 476–492, Apr. 1987.

[11] M. Vetterli, "A theory of multirate filter banks," *IEEE Trans. Acoust. Speech Signal Processing*, vol. ASSP-35, pp. 356–372, Mar. 1987.

[12] T. Q. Nguyen and P. P. Vaidyanathan, "Structures for M-channel perfect-reconstruction FIR QMF banks which yield linear-phase analysis filters," *IEEE Trans. Acoust. Speech Signal Processing*, pp. 433–446, Mar. 1990.

[13] T. A. Ramstad and J. P. Tanem, "Cosine-modulated analysis-synthesis filter bank with critical sampling and perfect reconstruction," in *Proc. IEEE Int. Conf. ASSP* (Toronto), May 1991, pp. 1789–1792.

[14] R. D. Koilpillai and P. P. Vaidyanathan, "New results of cosine-modulated FIR filter banks satisfying perfect reconstruction," in *Proc. IEEE Int. Conf. ASSP* (Toronto), May 1991, pp. 1793–1796.

[15] ——, "A spectral factorization approach to pseudo-QMF design," presented at the *IEEE Int. Symp. CAS*, Singapore, May 1991.

[16] ——, "New results on cosine-modulated FIR filter banks satisfying perfect reconstruction," Tech. Rep., Calif. Inst. Technol., Nov. 1990.

[17] H. S. Malvar, "Extended lapped transforms: Fast algorithms and applications," in *Proc. IEEE Int. Conf. ASSP* (Toronto), May 1991, pp. 1797–1800.

[18] D. F. Elliot, Ed., *Handbook of Digital Signal Processing, Engineering Applications*. San Diego, CA: Academic, 1987.

[19] P. P. Vaidyanathan and P. Q. Hoang, "Lattice structures for optimal design and robust implementation of two-channel perfect-reconstruction QMF banks," *IEEE Trans. Acoust. Speech Signal Processing*, pp. 81–94, Jan. 1988.

[20] J. H. Rothweiler, "Polyphase quadrature filters—A new subband coding technique," in *Proc. IEEE Int. Conf. ASSP* (Boston, MA), 1983, pp. 1280–1283.

[21] J. Mason and Z. Picel, "Flexible design of computationally efficient nearly perfect QMF filter banks," *IEEE Int. Conf. ASSP* (Tampa, FL), Mar. 1985, pp. 14.7.1–14.7.4.

[22] H. J. Nussbaumer, "Pseudo QMF filter bank," *IBM Tech. Disclosure Bull.*, vol. 24, pp. 3081–3087, Nov. 1981.

[23] R. V. Cox, "The design of uniformly and non-uniformly spaced pseudo-quadrature mirror filters," *IEEE Trans. Acoust. Speech Signal Processing*, vol. ASSP-34, pp. 1090–1096, Oct. 1986.

[24] F. Mintzer, "On half-band, third-band and Nth-band FIR filters and their design," *IEEE Trans. Acoust. Speech Signal Processing*, vol. ASSP-30, pp. 734–738, Oct. 1982.

[25] P. P. Vaidyanathan and T. Q. Nguyen, "A 'trick' for the design of FIR halfband filters," *IEEE Trans. Circuits Syst.*, vol. CAS-34, pp. 297–300, Mar. 1987.

[26] ——, "Eigenfilters: A new approach to least squares FIR filter design and applications including Nyquist filters," *IEEE Trans. Circuits Syst.*, vol. CAS-34, pp. 11–23, Jan. 1987.

[27] T. Q. Nguyen, "Eigenfilter for the design of linear-phase filters with arbitrary magnitude response," in *Proc. IEEE Conf. ASSP* (Toronto), May 1991, pp. 1981–1984.

[28] K. Schittkowski, "On the convergence of a sequential quadratic programming method with an augmented Lagrangian line search function," *Mathematik Operationsforschung und Statistik, Serie Optimization*, vol. 14, pp. 197–216, 1983.

[29] ——, "NLPQL: A FORTRAN subroutine solving constrained nonlinear programming problems," *Annals Oper. Res.* (C. L. Monma, Ed.), vol. 5, pp. 485–500, 1986.

[30] IMSL: A Mathematic Subroutine Package.

[31] M. G. Bellanger, G. Bonnerot, and M. Coudreuse, "Digital filtering by polyphase networks: Application to sample-rate alternation and filter banks," *IEEE Trans. Acoust. Speech Signal Processing*, vol. ASSP-24, pp. 109–114, Apr. 1976.

[32] J. H. McClellan, T. W. Parks, and L. R. Rabiner, "A computer program for designing optimum FIR linear phase digital filters," *IEEE Trans. Audio Electroacoust.*, vol. AU-21, pp. 506–526, Dec. 1973.

[33] J. Mau, "Perfect-reconstruction modulated filter banks," presented at the *IEEE Conf. ASSP*, 1992.

[34] H. S. Malvar, *Signal Processing with Lapped Transforms*. Boston, MA: Artech House, 1992.

[35] J. Princen and A. Bradley, "Analysis/synthesis filter bank design based on time domain aliasing cancellation," *IEEE Trans. Acoust. Speech Signal Processing*, pp. 1153–1161, Oct. 1986.

Truong Q. Nguyen (S'85–M'89) was born in Saigon , Vietnam, on November 2, 1962. He received the B.S. (Hons.), M.S., and Ph.D. degrees in electrical engineering from the California Institute of Technology, Pasadena, in 1985, 1986, and 1989, respectively.

Since June 1989, he has been with the Lincoln Laboratory of the Massachusetts Institute of Technology (MIT), Cambridge. During the academic year 1993–1994, he will be a visiting lecturer at MIT and an adjunct professor at Northeastern University, Boston, MA. His research interests are in digital signal processing, multirate systems and applications, filter design, ultrasonics nondestructive evaluation, and adaptive array processing.

Dr. Nguyen was a recipient of a fellowship from Aerojet dynamics for advanced studies during 1986–1987. He received the IEEE TRANSACTIONS ON SIGNAL PROCESSING 1992 Paper Award (Image and Multidimensional Processing Area) for the paper he co-wrote with P. P. Vaidyanathan on linear-phase perfect-reconstruction filter banks (March 1990). He is currently an Associate Editor for the IEEE TRANSACTIONS ON SIGNAL PROCESSING. He is a member of Tau Beta Pi, Eta Kappa Nu, and Sigma Xi.